Studies on Indian Silk. II. Structure–Property Correlations

Kushal Sen,[1] Murugesh Babu K[2]

[1]*Department of Textile Technology, Indian Institute of Technology, Hauz Khas, New Delhi 110 016, India*
[2]*Department of Textile Technology, Bapuji Institute of Engineering and Technology, Davangere 577 004, Karnataka, India*

Received 23 September 2002; accepted 12 October 2003

ABSTRACT: This second in a series of articles deals with studies on the structure and physical properties of five varieties of Indian silk: two mulberry (bivoltine and crossbreed) and three nonmulberry (tasar, muga, and eri). A detailed analysis of the microstructural parameters and mechanical properties was reported. Significant differences between and within the varieties with respect to microstructural parameters (crystallinity, density, birefringence, dichroic ratio, sonic modulus, etc.), as well as the effect of microstructural parameters on mechanical properties, were discussed. Some of the observations made on the inverse stress relaxation behavior of the different silk varieties were also reported. The extent of variation of these morphological parameters was found to correlate well with the mechanical properties. © 2004 Wiley Periodicals, Inc. J Appl Polym Sci 92: 1098–1115, 2004

Key words: silk; structure; mechanical properties; inverse stress relaxation; structure–property relations

INTRODUCTION

In the previous study in this series on Indian silk,[1] it was reported that the macrostructural characteristics of different varieties of silk, such as denier, filament length, cross section, and amino acid composition, are significantly different. In addition, it is interesting to note that large differences in the macrocharacteristics exist along the filament length within a cocoon of the same variety. Do these influence the microstructure and the mechanical properties of silk fibers? Can any correlation be established between structure and properties within a variety? These are some of the questions that need attention of the researchers.

Some of earlier investigators studied the physical properties and chemical architecture of some varieties of silk. Iizuka et al.[2–4] investigated some of the Japanese mulberry and Indian nonmulberry silk fibers. In these investigations, the emphasis was on the study of dependency of mechanical properties on the fiber denier. Their results revealed that the properties such as tenacity and dynamic modulus increased in all the varieties as the denier decreased; on the other hand, elongation at break showed a decreasing trend. A comparative study on the characteristics of filament from male and female cocoons of some of the Japanese mulberry silk was also reported.[5]

In a study on Indian mulberry and nonmulberry silk fibers treated with HCl of different concentrations for different durations, Bhat and Nadiger[6] reported that the microstrutural parameters, crystallinity and crystallite size, increased after the treatment. The crystallinity and crystal size of four Indian varieties of silk were studied using electron diffraction techniques.[7] They believed that some of the chains in the amorphous regions do crystallize after the treatment, perhaps onto the existing crystallites. The effect of plasma treatment on morphology and the surface characteristics of different varieties of Indian silk fibers were studied by Bhat and Ahirrao.[8]

The stress developed in a specimen, which is constrained to remain in its extended state, is known to decay with time, a process referred to as "stress relaxation." On the other hand, if an extended specimen is allowed to recover a part of the deformation given to it and is held at that level, it was shown that in some circumstances, the stress in the sample builds up with time. This phenomenon is termed as "inverse stress relaxation" (Ri).

Nachane et al.[9] studied the inverse stress relaxation and stress recovery behavior of cotton fibers and yarns and discussed the mechanism of inverse stress relaxation behavior. Similar studies were conducted by the above authors on cotton fibers and yarns, ramie, wool, poly(ethylene terephthalate), and viscose.[10,11] Some other studies also reported on the inverse stress relaxation of spun yarns of cotton, polyester, viscose, jute,[12–14] and polypropylene.[15] Silk is also a viscoelastic material and is expected to exhibit the phenomenon of inverse stress relaxation; mulberry and tasar silk fibers were previously studied in this respect.[16] In the above study, it was reported that the inverse stress

Correspondence to: M. Babu K.

Journal of Applied Polymer Science, Vol. 92, 1098–1115 (2004)

TABLE I
Average Tenacity, Elongation, and Initial Modulus Values of Silk

Variety	Tenacity[a] (g/d)	Elongation at break[a] (%)	Initial modulus[a] (g/d)
Mulberry (bivoltine)	3.75	13.5	95
Mulberry (crossbreed)	3.85	16.1	107
Tasar	4.50	26.5	84
Muga	4.35	22.3	81
Eri	3.70	20.8	89

[a] Average of outer and inner layers.

relaxation increases with the increase in the initially applied tension. Cyclic loading was found to reduce the extent of inverse stress relaxation.

Although the previous studies were aimed at analyzing the properties and the structure of individual silk fibers, a detailed study on the correlation of the structure with the properties has not been reported to date. In addition, the investigations were isolated and a comprehensive study on all the varieties of Indian silk is not available. In particular, investigative studies on the structure and properties of muga and eri silks are very limited. It was thus considered of interest to study in detail the physical properties of different varieties of silk and to find whether a general correlation exists between the mechanical properties and microstructural parameters such as crystallinity, crystallite size, birefringence, and sonic modulus, for example. An attempt was also made to study the time-dependent stress relaxation and inverse stress relaxation behavior of silk fibers. Of particular interest are the properties along the filament length within a cocoon.

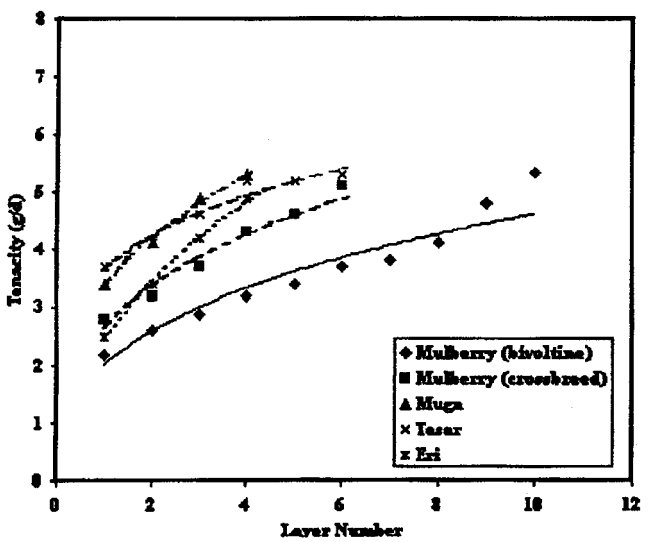

Figure 1 Tenacity along the layers.

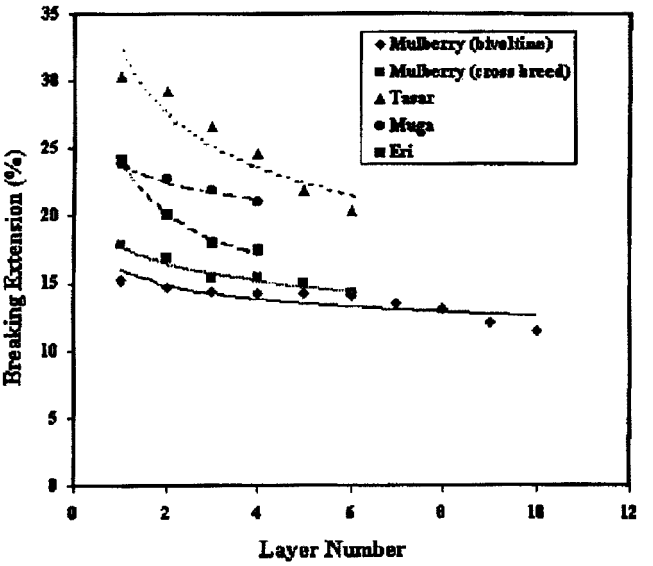

Figure 2 Breaking extension along the layers.

EXPERIMENTAL

Materials

The raw materials—cocoons of mulberry, tasar, muga, and eri—were chosen for the present study.

Sample preparation

The reeled and degummed samples were prepared and suitably numbered according to the procedure given in the previous study.[1]

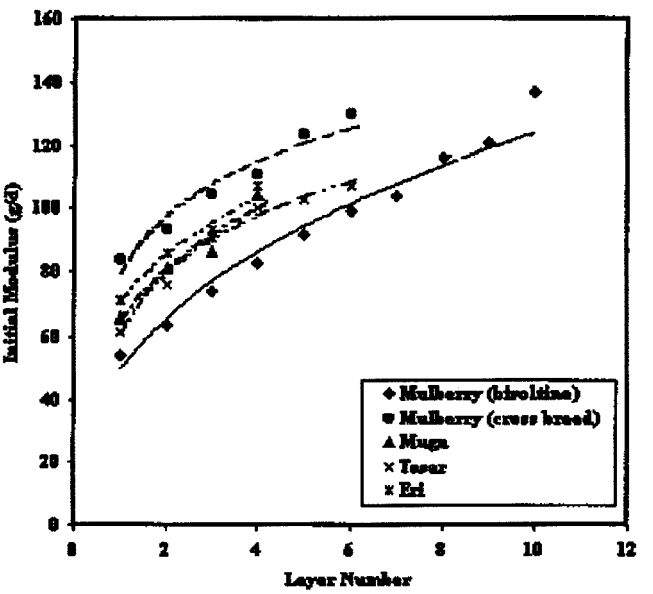

Figure 3 Initial modulus along the layers.

Preparation of amorphous sample

The degummed mulberry silk fibers were dissolved in a solution of ethanol, water, and calcium chloride in the ratio of 5 : 6 : 8, respectively, at a temperature of 50°C for 1 h. Similarly, the nonmulberry fibers were dissolved in 9*M* lithium bromide solution at 70°C for 1 h. The silk fibroin was coagulated using water, then dried and ground to a fine powder. This amorphous powder sample was taken as the reference sample for WAXD studies. Separate amorphous curves were obtained for each silk.

Evaluation

Mechanical properties

The mechanical properties (tenacity, elongation at break, and initial modulus) of single filaments were determined on Instron Tensile Tester (Model 4301; Instron, Canton, MA) at standard conditions of 27 ± 2°C and 65% relative humidity. The tests were conducted under the following specifications: gauge length, 50 mm; crosshead speed, 50 mm/min; pretension, 0.04 g/d.

An average was taken from 40 readings.

Determination of inverse stress relaxation index (Ri)

An Instron tensile tester model 1112 (Instron, Canton. MA) was used for the determination of Ri. The experiment consisted of stretching the specimen, allowing it to retract partially, and then observing the stress build up over a period of time.

Based on preliminary tensile test data the specimens were loaded to a level just below the yield point (85% of the load at which the specimen starts yielding). From this level, they were allowed to retract to preselected load levels (20, 40, 60, and 80% of the peak load W_1; see Fig. 1 and the change in tension with time was recorded for each retraction level. The test specifications were as follows: gauge length, 50 mm; crosshead speed, 50 mm/min; pretension, 0.04 g/d; chart speed, 20 mm/min.

The inverse stress relaxation was determined by an index referred to as "inverse stress relaxation index," and was calculated as follows:

Inverse stress relaxation index (Ri)

$$= \frac{W_3 - W_2}{W_1} \times 100$$

where W_3 is the final load, W_2 is the load at time t_2, and W_1 is the initial load (see Fig. 6).

A special case where the retraction level is zero is a classical stress relaxation experiment. It is obvious that for such a case Ri will assume a negative value.

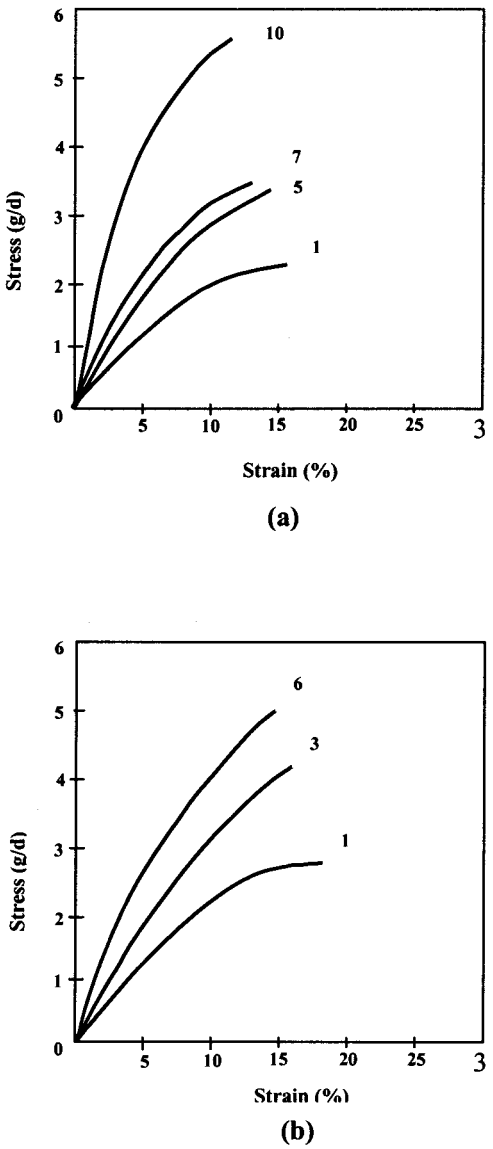

Figure 4 Stress–strain curves of mulberry silks: (a) bivoltine; (b) crossbreed. (The numbers assigned to the curves represent the layer numbers.)

Fiber characterization

X-ray crystallinity

WAXS diffractograms of powdered silk fiber sample and amorphous silk samples were taken using an X-ray generator (Philips, The Netherlands). Ni-filtered Cu–K_α (1.54 Å) radiation was used at 40 kV and 20 mA. The samples were scanned between 10 and 35° (2θ values). The percentage crystallinity was determined as

$$\text{Crystallinity (\%)} = [1 - (A_a/A_t)] \times 100$$

where A_a and A_t are the integrated areas of the amorphous sample and sample fiber diffractograms, respectively.

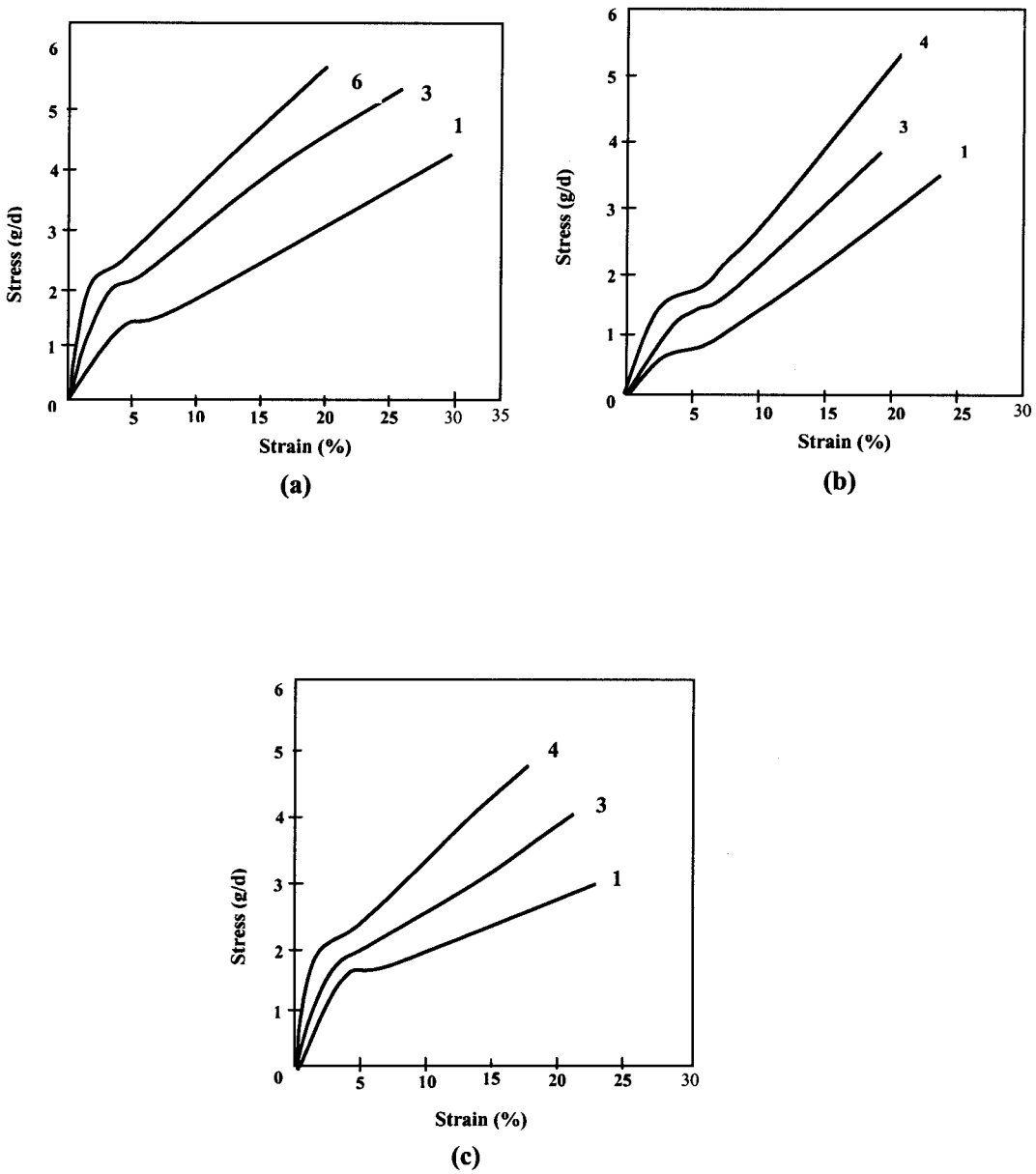

Figure 5 Stress–strain curves of nonmulberry silks: (a) tasar; (b) muga; (c) eri. (The numbers assigned to the curves represent the layer numbers.)

Crystallite size

The crystallite size (W) was determined using the Scherrer formula[17]

$$W = K\lambda/\beta \cos \theta$$

where K is the shape factor, taken as unity; $\lambda = 1.54$ Å for Cu–K_α radiation; and β is the width of diffraction peak in radians at half intensity.

Crystallite orientation function (f_c)

Using a parallel bundle of silk filaments the crystallite orientation function was determined from azimuthal intensity distribution curves using Herman's orientation function as follows:

$$f_c = \frac{1}{2}[3\langle \cos^2\phi \rangle - 1]$$

where ϕ is the angle between the reference direction (filament axis) and the X-crystallographic axis. Assuming rotational symmetry about the filament axis

$$\langle \cos^2\phi \rangle = \frac{\Sigma I(\phi) \sin \phi \cos^2\phi \, d\phi}{\Sigma I(\phi) \sin \phi d\phi}$$

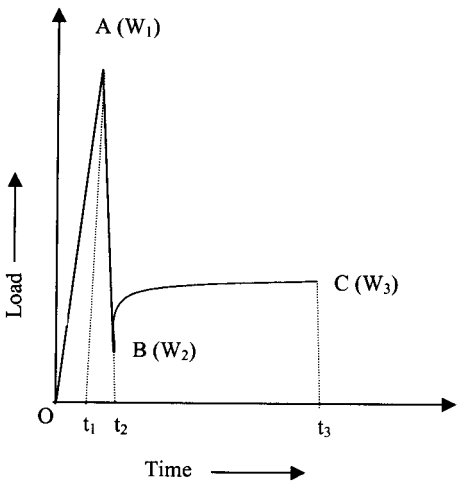

Figure 6 Typical curve showing the inverse stress relaxation behavior.

where $I(\phi)$ is the intensity diffracted from the $(h\,k\,l)$ planes, which are normal to the X-crystallographic direction.

FTIR–dichroic ratio

A Jasco FTIR spectrometer (model Micro FTIR 200; Jasco, Tokyo, Japan) was used for infrared analysis. FTIR absorption spectra of a small bundle of filaments were recorded from 800 to 1400 cm^{-1}. In all cases, 16 scans were averaged, keeping a resolution of 4 cm^{-1}. The dichroic ratio (D) was determined from the ratio of absorption intensities of spectra with the polarizer angle at 0° ($A_{\parallel}$, parallel to fiber axis) and that at 90° ($A_{\perp}$, perpendicular to fiber axis). D ($A_{\parallel}/A_{\perp}$) was calculated at wavenumbers 999.25 and 976.10 cm^{-1} for the mulberry varieties and at 965.49 cm^{-1} for all three nonmulberry varieties.

Birefringence

The Beckeline method was used for determination of the birefringence. A series of mixtures using two liquids [i.e., liquid paraffin (refractive index, $\eta = 1.465$) and 1-chloronaphthaline ($\eta = 1.633$)] were prepared for determination of the refractive index of single filaments in both the parallel and the perpendicular directions. The refractive index of the mixture, in which the Beckeline vanished under a polarizing microscope, was taken as the refractive index of fiber. The birefringence (Δ_n) was calculated using the relation

$$\Delta_n = \eta_{\parallel} - \eta_{\perp}$$

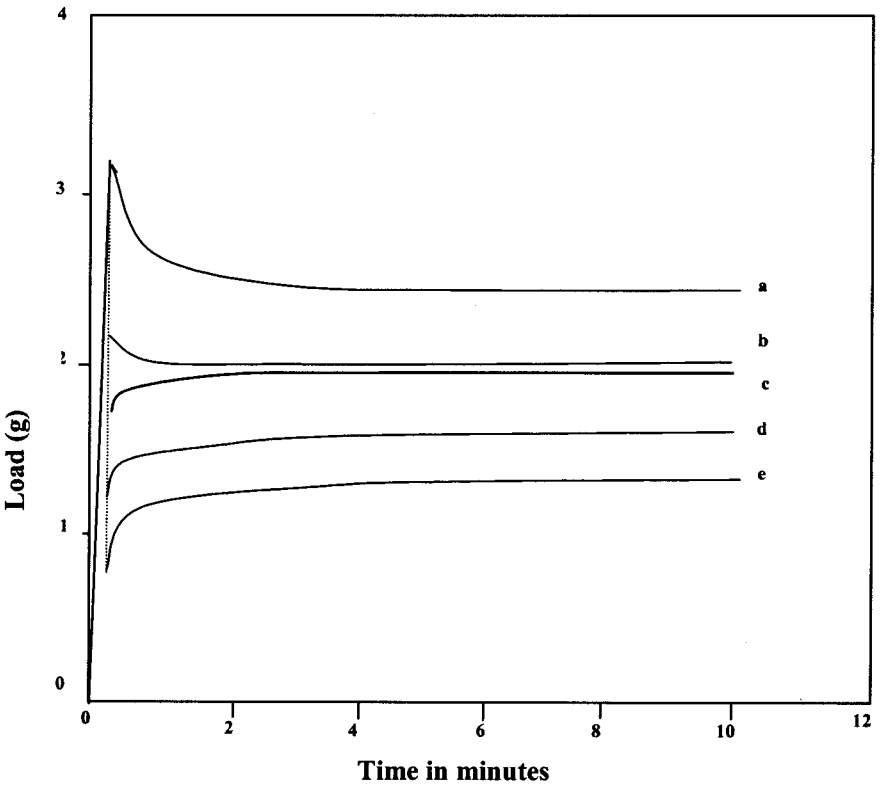

Figure 7 Inverse stress relaxation in mulberry (bivoltine; outer layer) silk fibers at different levels of retraction: (a) 0%; (b) 20%; (c) 40%; (d) 60%; (e) 80%.

TABLE II
Ri Values for Different Varieties of Silk Fibers

	Mulberry (bivoltine)		Mulberry (crossbreed)		Tasar		Muga		Eri	
Retraction level (%)	Outer layer	Inner layer	Outer layer	Inner layer	Outer layer	Inner layer	Outer layer	Inner layer	Outer layer	Inner layer
0	−23.7	−16.1	−25.0	−18.7	−39.0	−33.4	−24.6	−22.6	−28.1	−24.4
20	−7.6	−0.6	−4.0	−3.3	−11.3	−9.4	−11.6	−8.3	−15.0	−10.0
40	7.7	7.0	10.0	8.3	5.4	3.8	6.6	5.8	6.3	5.3
60	8.3	6.7	13.3	10.0	15.0	12.5	11.7	8.0	9.3	7.5
80	16.7	11.7	17.3	12.2	23.8	20.0	21.8	15.0	15.0	11.7

where $\eta_{\parallel}$ is the refractive index of the fiber in the parallel direction and $\eta_{\perp}$ is the refractive index of the fiber in the perpendicular direction to the plane of the polarizer light. An average of five readings was reported.

Sonic modulus

The sonic modulus of the single filament was measured using a dynamic modulus tester PPM-5 using the formula

$$E = 11.3Y^2$$

where E is the sonic modulus (in g/d) and Y is the sonic velocity (in km/s). An average obtained from 10 filament samples was reported.

RESULTS AND DISCUSSION

Mechanical properties

The mechanical properties such as tenacity, elongation at break, and initial modulus for different varieties of Indian silk were measured and were found to show interesting differences that provide the basis for the present discussion. It may be observed from Table I that the average tenacity of mulberry (bivoltine) is 3.75 g/d and that of mulberry (crossbreed) is 3.85 g/d. On the other hand, among the three nonmulberry varieties, tasar shows the highest average tenacity of 4.5 g/d followed by muga (4.35 g/d) and eri (3.7 g/d). The average value of tenacity is a misleading value. One may note that the tenacity values increase substantially along the filament length within a cocoon as one

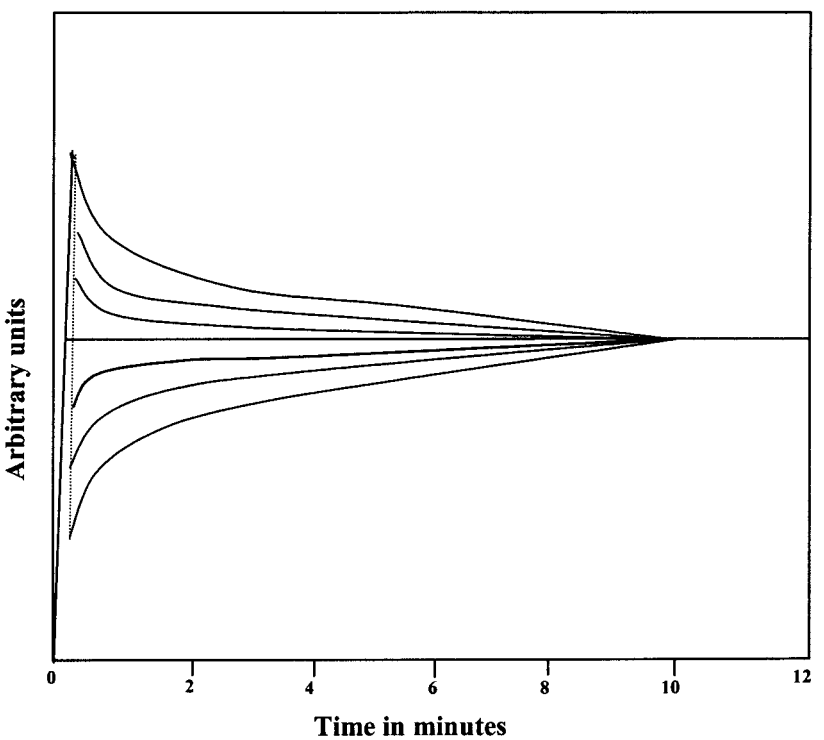

Figure 8 Typical theoretical curve depicting the inverse stress relaxation behavior.

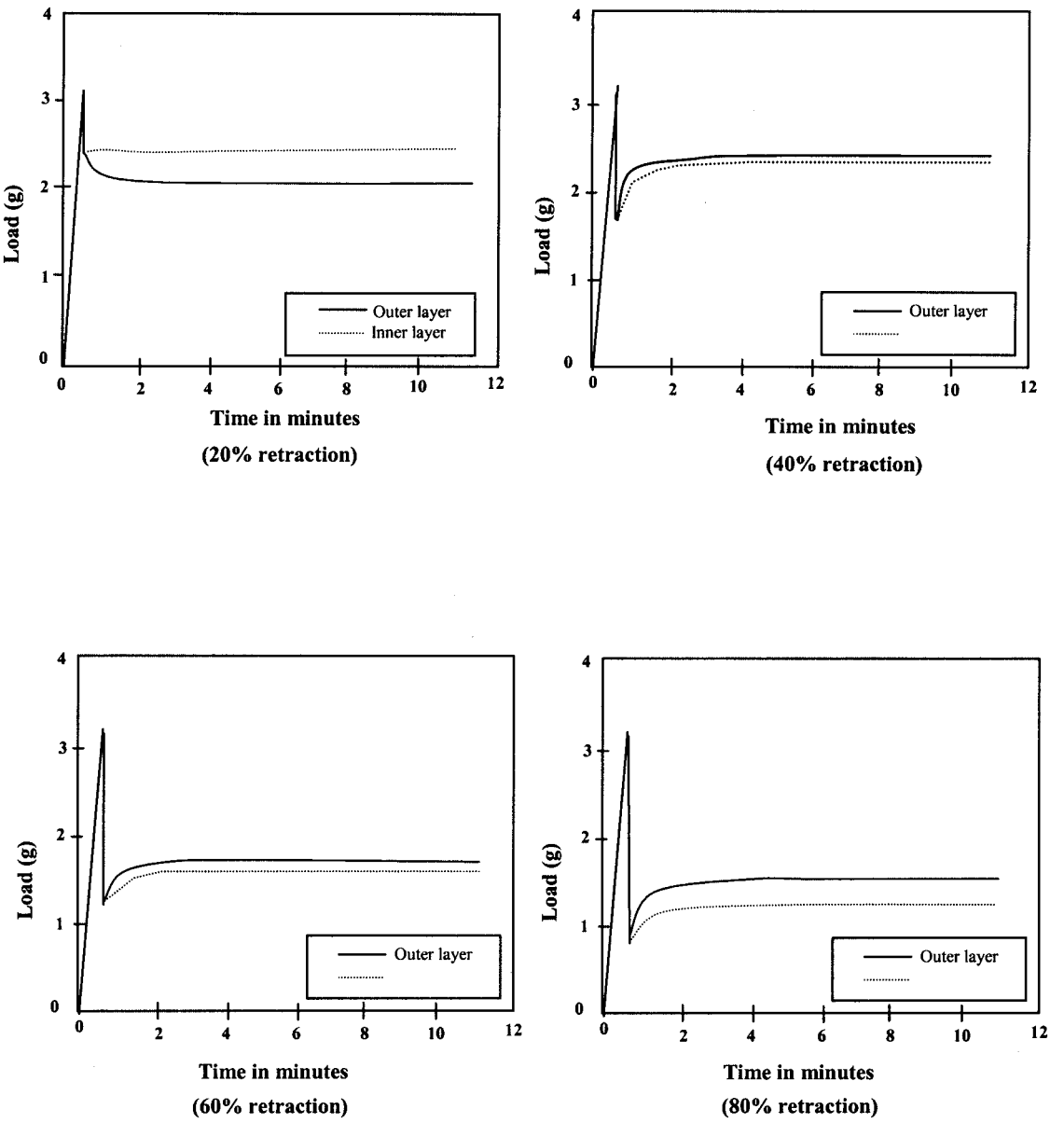

Figure 9 Inverse stress relaxation behavior of mulberry (bivoltine) silk fibers at different levels of retraction.

moves from the outer to the inner layers. This is true for all the varieties. The tenacity values range from 2.2 to 5.3 g/d ($\Delta_{ten} \approx 245\%$) for mulberry (bivoltine), 2.8 to 4.9 g/d ($\Delta_{ten} \approx 189\%$) for mulberry (crossbreed), 3.4 to 5.3 g/d ($\Delta_{ten} \approx 155\%$) for muga, 3.7 to 5.3 g/d ($\Delta_{ten} \approx 143\%$) for tasar, and 2.5 to 4.9 g/d ($\Delta_{ten} \approx 196\%$) for eri (Fig. 1). This means that, depending on the position and size of the test sample, one may obtain values that may be quite different from those expected. The total percentage increase in tenacity may give an impression that mulberry (bivoltine) has the maximum variation along the length, but this could also be a misrepresentation because the filament length in all the varieties is not the same; in fact it is quite different. Another way to look at this change is to view percentage change per unit length. The percentage increase per 100 m of the filament is around 0.222 for mulberry (bivoltine), 0.286 for mulberry (crossbreed), 0.235 for

TABLE III
Registered Tension (g) after 10 Minutes

	0% Retraction		80% Retraction	
Variety	Outer layer	Inner layer	Outer layer	Inner layer
Mulberry (bivoltine)	2.44	2.70	1.10	0.95
Mulberry (crossbreed)	2.40	2.60	1.10	0.91
Tasar	4.88	5.33	3.20	3.00
Muga	4.52	4.64	2.43	2.00
Eri	2.30	2.42	1.38	1.20

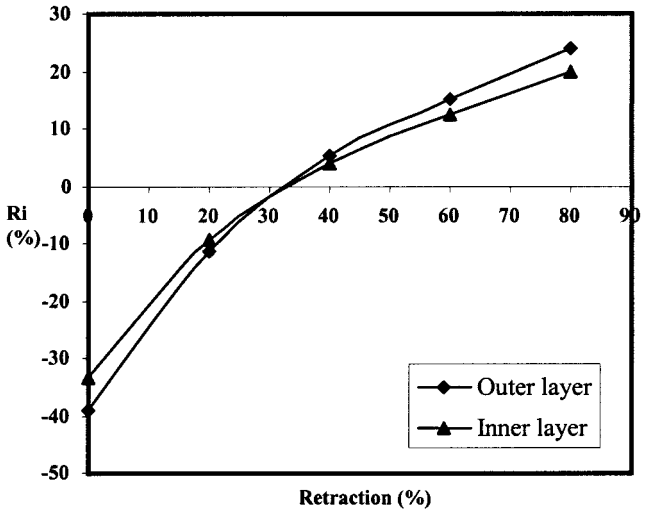

Figure 10 Ri versus retraction level (tasar).

tasar, 0.325 for muga, and 0.445 for eri. This clearly indicates that the variation in mulberry is not all that high, making eri the most nonuniform in terms of tenacity along the fiber. This definitely confirms that, although all the mechanical properties change substantially all along the length, they follow a definite trend.

Breaking extension values show a reverse trend compared to that of tenacity. Interestingly, higher breaking extension values were observed for nonmulberry silks. There is a substantial reduction in the extension values along the filament length from the outer to the inner layers. The values for mulberry varieties vary from 15.3 to 11.8% for mulberry (bivoltine) and 17.8 to 14.4% for mulberry (crossbreed). On the other hand, the extension values ranged between 23.8 to 20.9% for muga, 30.4 to 22.6% for tasar, and 24.1 to 17.5% for eri (Fig. 2).

Two points are worth noting: (1) the reduction in extension values is much less compared to the increase in tenacity and (2) the average extension values of nonmulberry varieties are much higher than those of the mulberry varieties (in all cases a high CV% values ranging from 18.5 to 34.1% were observed). The relatively high degree of extension in the case of nonmulberry silks may be attributed to the following: (1) All the nonmulberry silks contain more amino acid residues with bulky side groups than the mulberry silk varieties.[18] This enables molecular chains in noncrystalline regions in the fiber structure to slip easily when stretched and thus show higher elongation at break. (2) Unfolding of the long fibroin chains in the amorphous regions is a result of either less orientation or less crystallinity.[19–21]

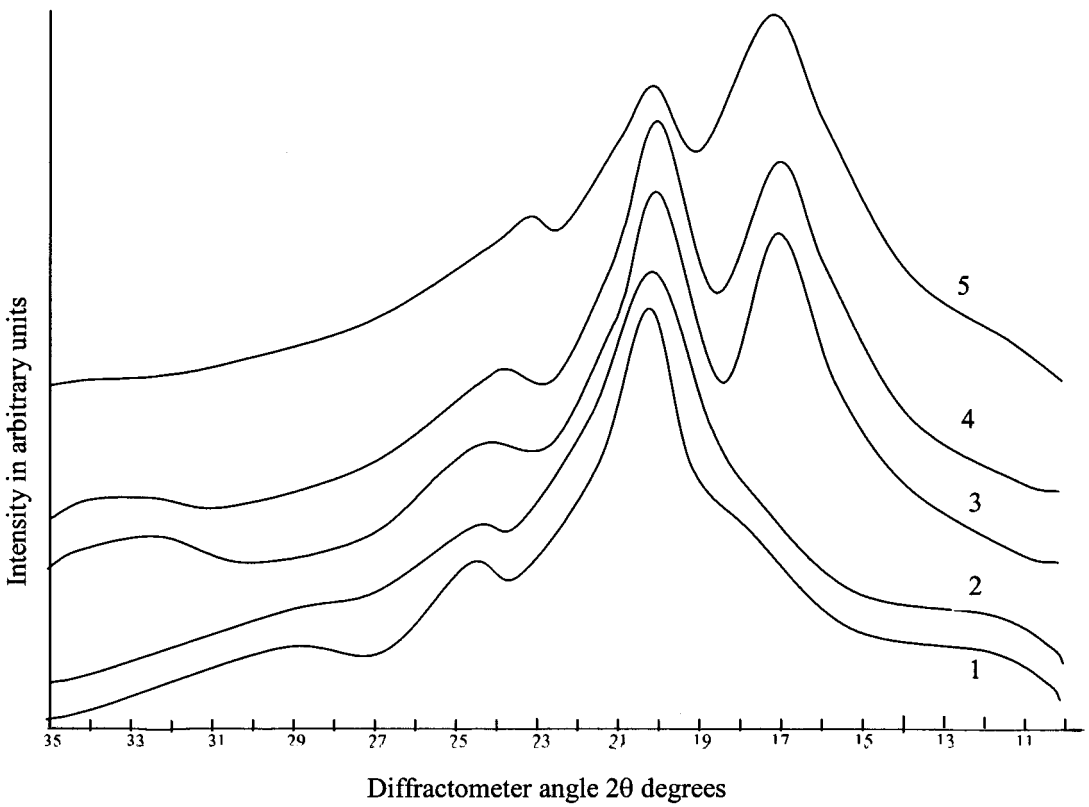

Figure 11 WAXD spectra of mulberry and nonmulberry silk fibers: (1) mulberry (bivoltine); (2) mulberry (crossbreed); (3) tasar; (4) muga; (5) eri.

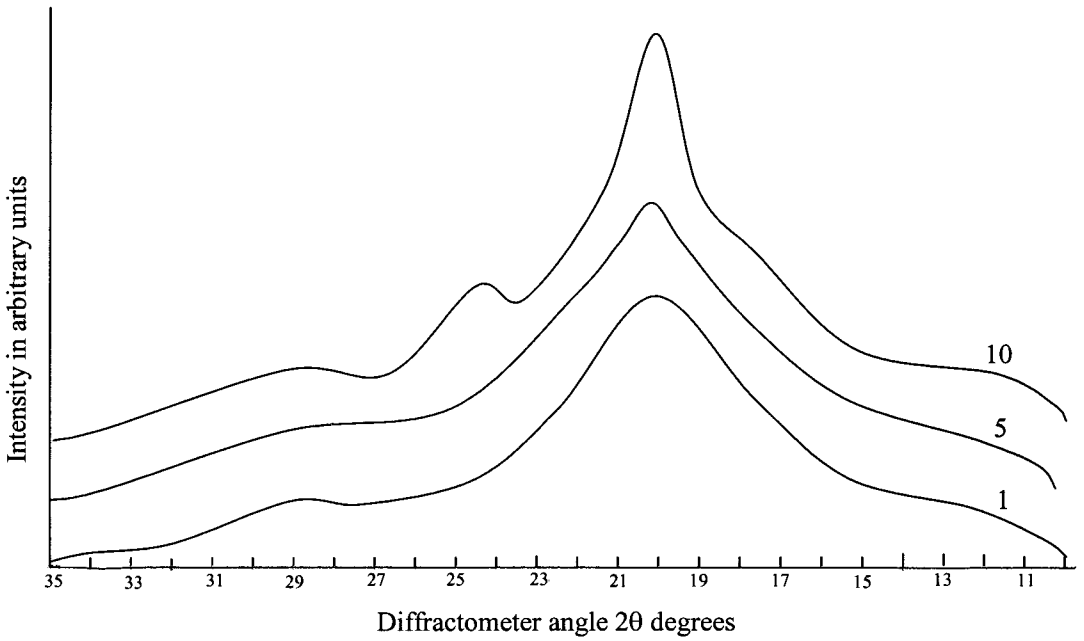

Figure 12 WAXD spectra of mulberry (bivoltine) silk fibers. (The numbers assigned to the curves represent the layer numbers.)

Another important tensile parameter is the initial modulus. The initial modulus values for different varieties and its change along the filament length are plotted in Figure 3. The initial modulus values follow a similar trend as that of tenacity, showing higher values for the inner layers. The values ranged between 53.9 and 136.8 g/d for mulberry (bivoltine), 83.8 and 129.8 g/d for mulberry (crossbreed), 61.3 and 100.7 g/d for muga, 61.4 and 107 g/d for tasar, and 71.1 and 107 g/d for eri silks. This definitely indicates an increase in orientation, in both the crystalline and the amorphous regions, as one moves from the outer to the inner layers.

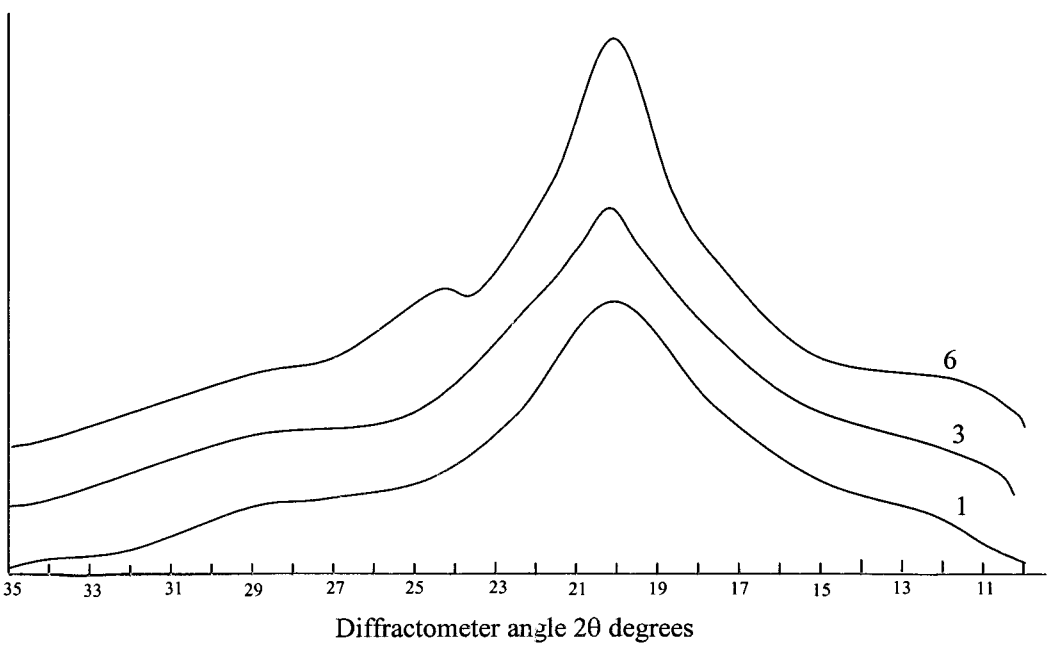

Figure 13 WAXD spectra of mulberry (crossbreed) silk fibers. (The numbers assigned to the curves represent the layer numbers.)

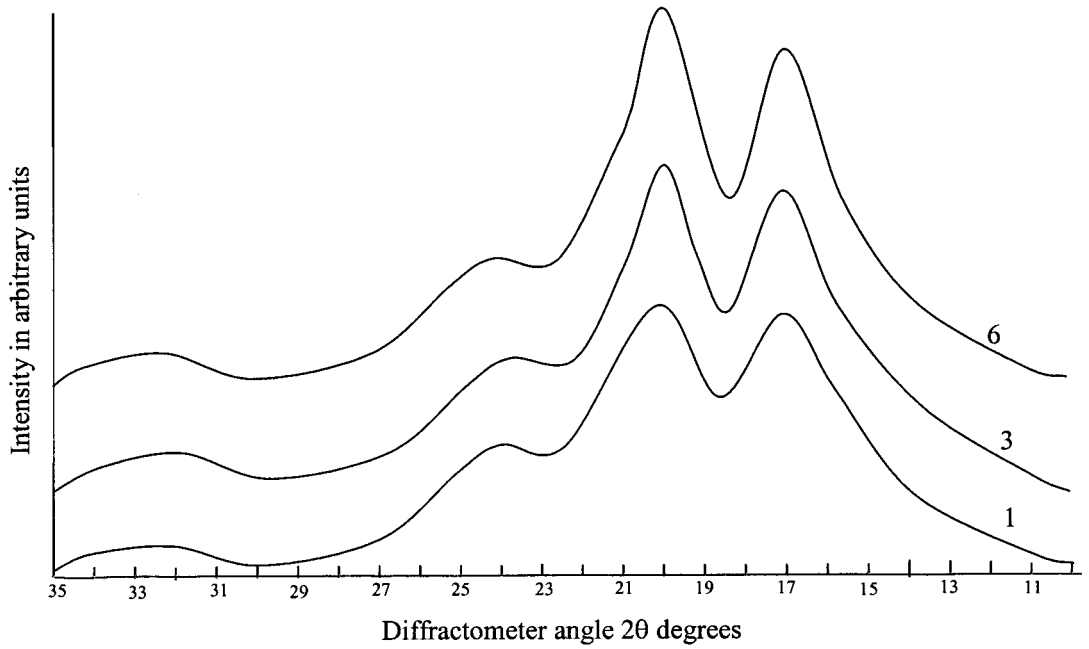

Figure 14 WAXD spectra of tasar silk fibers. (The numbers assigned to the curves represent the layer numbers.)

To gain further insight, it was considered worthwhile to analyze the stress–strain behavior of these varieties. It may be noted that the curves for both the mulberry silks (Fig. 4) do not show any well-defined yield point. In addition, the finer the filament becomes (i.e., as one moves from the outer to the inner layers), the higher the tenacity and modulus and the lower the elongation at break. Interestingly, a sharp yield point at a strain level of about 2 to 3% may be observed for all the nonmulberry silk fibers (Fig. 5). Following the yield point, the flow region continues up to 7% strain, depending on the fineness. This region is followed by a strain-hardening region, which was not observed in mulberry silk. This behavior suggests that mulberry varieties have well-developed crystalline regions that are responsible for smaller and gradual elongation with increasing stress. Tasar, muga, and eri, on the other hand, demonstrate a high initial resistance to

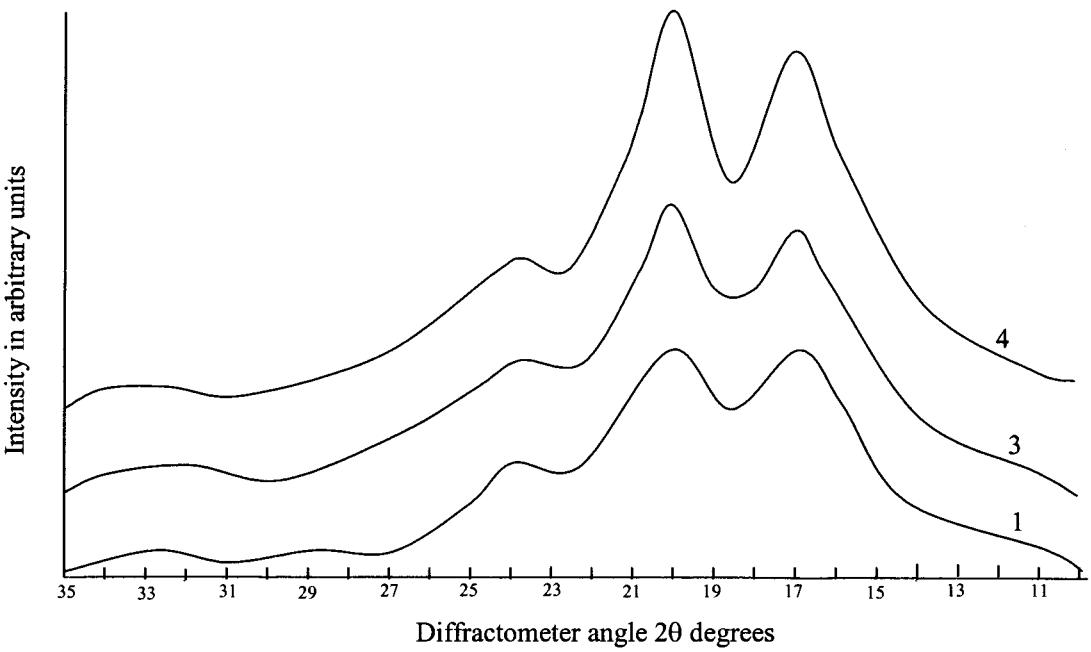

Figure 15 WAXD spectra of muga silk fibers. (The numbers assigned to the curves represent the layer numbers.)

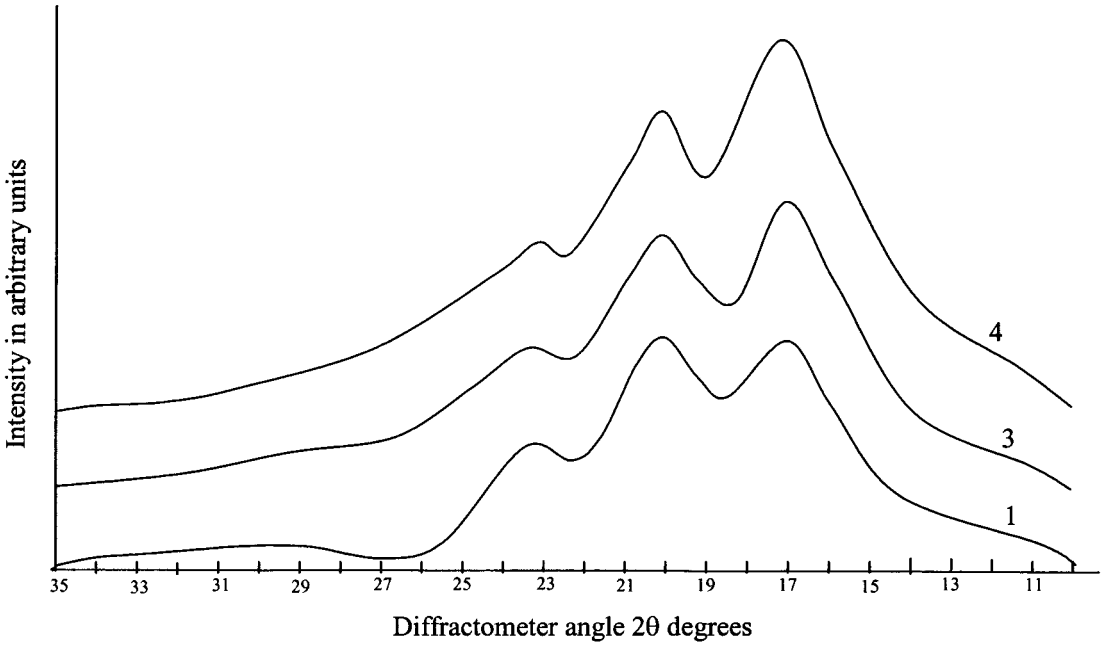

Figure 16 WAXD spectra of eri silk fibers. (The numbers assigned to the curves represent the layer numbers.)

deformation followed by substantial yielding. This suggests two things: (1) fewer crystalline regions; and (2) imperfect crystallites or entanglements, which initially offer resistance but later give way and allow easy deformation in the amorphous regions until strain hardening occurs.

Stress relaxation and inverse stress relaxation

Inverse stress relaxation is an important viscoelastic response of the fiber because it reflects the textile material's behavior during processing and actual use, particularly that related to dimensional stability and resilience. Figure 6 shows the typical curve demonstrating inverse stress relaxation: OA represents the rise in load resulting from the initial stretching, AB is the retraction, and BC is the stress build up with time.

Typical stress relaxation and inverse stress relaxation behaviors of mulberry (bivoltine) silk (outer layer) are shown in Figure 7. It is interesting to note that, depending on the retraction level of load, the phenomenon represents either the stress relaxation or the inverse stress relaxation phenomenon. It may be observed from these curves that at retraction levels of

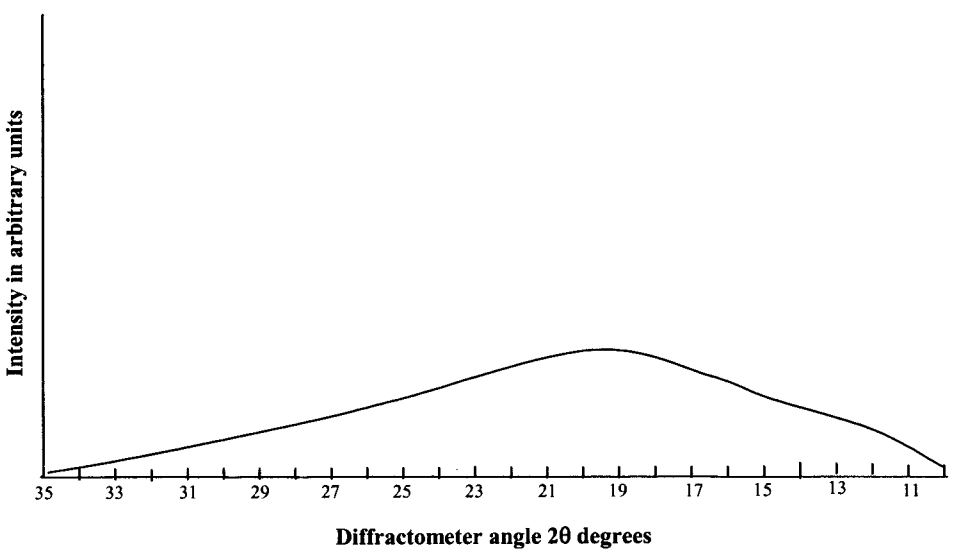

Figure 17 WAXD spectrum of amorphous silk.

TABLE IV
X-ray Crystallinity Values for Different Varieties of Silks

Type of silk	X_c (%)		
	Outer layer	Middle layer	Inner layer
Mulberry (bivoltine)	29.2	37.8	48.8
Mulberry (crossbreed)	28.1	34.9	47.2
Tasar	28.9	30.9	45.7
Muga	26.9	32.4	45.8
Eri	24.2	30.1	43.6

TABLE VI
Crystallite Orientation Function (f_c) Values for Different Varieties of Silks

Type of silk	f_c		
	Outer layer	Middle layer	Inner layer
Mulberry (bivoltine)	0.40	0.44	0.49
Mulberry (crossbreed)	0.32	0.36	0.41
Tasar	0.32	0.35	0.42
Muga	0.35	0.38	0.43
Eri	0.23	0.26	0.28

0 and 20%, the fiber shows stress relaxation and gives a negative Ri value (Table II). At retraction levels of 40, 60, and 80%, however, one observes the inverse stress relaxation phenomenon (i.e., one observes stress build-up). As can be seen from the values given in the tables, the Ri begins with a relatively high negative value at a low retraction level (0 and 20% in the present case, signifying stress relaxation) and becomes increasingly more positive for higher values of retraction, with Ri showing the highest value of 16.7 at a level of 80%. This type of behavior was observed in all the varieties of silk fibers (Table II).

Among the two mulberry varieties, the mulberry (crossbreed) variety shows higher Ri values compared to those of the mulberry (bivoltine) variety. For instance at an 80% retraction level, mulberry (crossbreed) shows an Ri value of 17.3 (outer layer) as against 16.7 (outer layer) for the mulberry (bivoltine) variety. It is evident from earlier studies[18] that mulberry (crossbreed) shows lower crystallinity and crystallite orientation compared to those of the mulberry (bivoltine) variety. This leads to easy unfolding and molecular relaxation of chains in the amorphous regions, and in general also results in higher stress relaxation as the stress builds up with time.

It is quite clear from the Figure 7 that, whether it is stress relaxation or inverse stress relaxation, both involve molecular rearrangement in a way that achieves lower internal energy within the fiber system. The molecular relaxation involves disorientation and coiling up because this state is thermodynamically favorable (i.e., it leads to an increase in entropy), particularly in the amorphous region. The inverse stress relaxation is a process akin to shrinkage. If the fiber is constrained (i.e., not allowed to shrink), then shrinkage stress builds up. As mentioned previously, silk, like any other textile fiber, is a viscoelastic material and undergoes a time-dependent relaxation process. When after stressing to a reasonably high stress level, a sudden decrease in stress level (i.e., retraction) to a level more than it would normally have achieved, in practical time limits, realizes what one may call virtual slackness, and thus may tend to show a shrinkage tendency to achieve thermodynamically stable configuration. In the present case, because the fiber was not allowed to shrink, the stress built up until some equilibrium distribution of stress was achieved.

Figure 7 shows a typical curve for mulberry (bivoltine) silk. One would have expected all these curves, those representing stress relaxation or inverse stress relaxation, to theoretically meet at a unique point; that is, at a retraction level where the inversion occurs (Fig. 8). However, as one may see this does not happen (Fig. 7). The curve at the 0% retraction level ends up at higher stress level compared to that at 20%, and so on. This means that one obtains a band where the final

TABLE V
Crystallite Size Values for Different Varieties of Silks

Type of silk	Crystallite size (Å)		
	Outer layer	Middle layer	Inner layer
Mulberry (bivoltine)	19.4	22.3	23.5
Mulberry (crossbreed)	17.9	18.6	22.3
Tasar	26.5	28.4	29.9
Muga	23.7	26.5	27.9
Eri	31.9	34.4	35.8

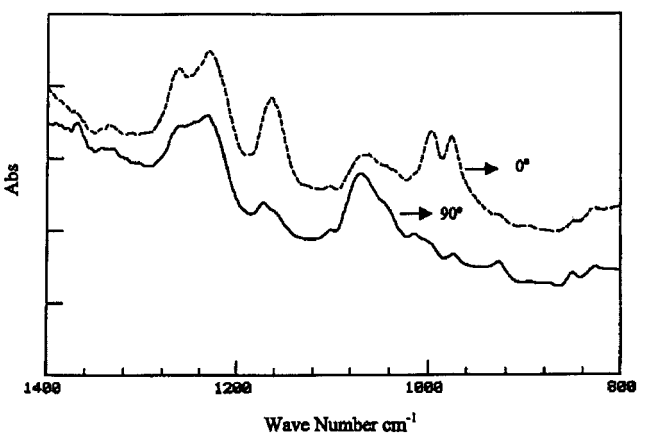

Figure 18 FTIR spectra of mulberry (bivoltine) silk fibers showing the difference in absorption intensities when the polarizer angle is at 0 and 90°.

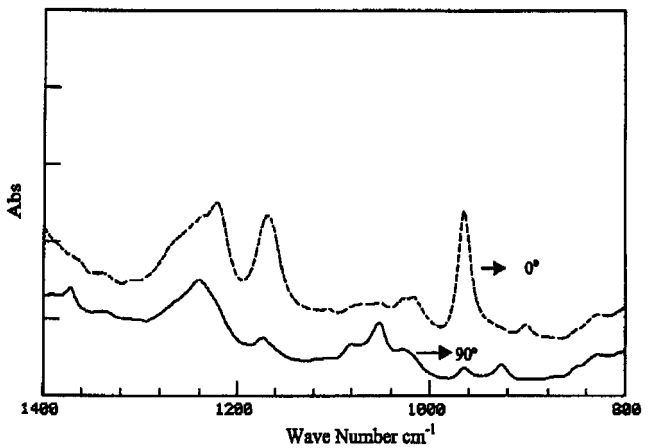

Figure 19 FTIR spectra of eri silk fibers showing the difference in absorption intensities when the polarizer angle is at 0 and 90°.

stress level may become constant, depending on the initial stress and the retraction level. Both the mechanical stressing and the retraction lead to some molecular slippage, of course constrained by the crystalline fraction and its nature. This constraint may be called the frictional set that does not allow full relaxation and thus molecular chains can rearrange only to certain permitted levels. This is what is designated as the final stress level. The morphology of the fiber thus has a significant role to play in the relaxation process.

In this respect the nonmulberry silk varieties also behave in a similar manner: (1) All these varieties show stress relaxation and inverse stress relaxation phenomena, depending on the retraction level (Table II). The Ri changes from an extreme negative value to a value that is more positive as the retraction level is changed from 0 to 80%. (2) All these varieties show a band where stress levels stabilize, that is, the highest stress level for 0% retraction and the lowest for 80% retraction in the present study. It is imperative in all the cases that if retraction levels are further decreased, the stress may stabilize at still lower levels at equilibrium.

TABLE VII
FTIR–Dichroic Ratio (*D*) for Different Varieties of Silks

Type of silk	*D*		
	Outer layer[a]	Middle layer	Inner layer
Mulberry (bivoltine)	1.34 (999.25 cm^{-1})	1.43	1.44
	1.38 (976.10 cm^{-1})	1.47	1.49
Mulberry (crossbreed)	1.23 (999.25 cm^{-1})	1.31	1.42
	1.27 (976.10 cm^{-1})	1.36	1.49
Tasar	1.38 (965.49 cm^{-1})	1.47	1.48
Muga	1.31 (965.49 cm^{-1})	1.43	1.45
Eri	1.21 (965.49 cm^{-1})	1.38	1.42

[a] Figures in parentheses represent the wavenumber at which dichroic ratio was calculated.

TABLE VIII
Birefringence Δ_n Values for Different Varieties of Silks

Type of silk	Δ_n		
	Outer layer	Middle layer	Inner layer
Mulberry (bivoltine)	0.054	0.055	0.056
Mulberry (crossbreed)	0.051	0.052	0.052
Tasar	0.041	0.042	0.042
Muga	0.040	0.041	0.042
Eri	0.034	0.035	0.035

It is interesting to note, however, that in general the Ri values for nonmulberry varieties are higher than those for mulberry varieties. For instance, at 0% retraction, Ri (%) for tasar is more negative (39.0–33.4) compared to mulberry (23.7–16.1) and at 80% is more positive (i.e., ~ 23.8–20.0) (Fig. 5), which further substantiates the fact that the lower the morphological order, the higher the likely value of Ri. In the previous study, it was shown that the crystallinity and orientation in nonmulberry varieties are lower.[18]

It is also interesting to note that Ri values obtained for the outer layers are always greater than those obtained for the inner layers, irrespective of the type of silk. It may be recalled that the microstructural parameters such as crystallinity, crystallite orientation, birefringence, and so forth, show an increase as one moves from the outer to the inner layers,[18] suggesting that the more ordered molecular arrangement in the inner layers does not allow free and easy relaxation of molecules, resulting in lower stress relaxation and stress build up. Figure 9 shows typical curves for mulberry (bivoltine) representing the outer and inner layers, which clearly emphasizes the point mentioned above. This is also clear from the final tension (g) registered for the inner and outer layers (Table III).

Figure 10 shows a typical graph that represents the effect of retraction level on the Ri values of tasar fibers. It may be observed that the retraction level at which the Ri becomes zero is identical, at around 32% for the outer and the inner layers. Similarly, it is around 25%

TABLE IX
Sonic Modulus S_ε Values for Different Varieties of Silks

Type of silk	S_ε (g/d)		
	Outer layer	Middle layer	Inner layer
Mulberry (bivoltine)	165	170	206
Mulberry (crossbreed)	153	167	192
Tasar	106	107	115
Muga	103	108	114
Eri	101	106	109

TABLE X
Correlation Coefficient *R* Value Between Tenacity and Microstructural Parameters

Within variety	Crystallinity (X_c)	Crystallite orientation function (f_c)	Crystallite size	Birefringence (Δ_n)	Sonic modulus (S_ε)	Dichroic ratio (D)
Mulberry (bivoltine)	0.92 (+)	0.913 (+)	0.961 (+)	0.869 (+)	0.690 (−)	0.980 (+)
Mulberry (crossbreed)	0.935 (+)	0.921 (+)	0.963 (+)	0.743 (+)	0.924 (+)	0.902 (+)
Tasar	0.919 (+)	0.992 (+)	0.988 (+)	0.974 (+)	0.878 (+)	0.989 (+)
Muga	0.978	0.966	0.950	0.943	0.959	0.988
Eri	0.945 (+)	0.924 (+)	0.958 (+)	0.864 (+)	0.939 (+)	0.869 (+)
Global	0.877 (+)	0.622 (+)	0.193 (+)	0.145 (+)	0.209 (+)	0.840 (+)

for mulberry (crossbreed), 23–28% for mulberry (bivoltine), 30–32% for muga, and 32–33% for eri.

WAXD studies

In keeping with the theme of the present study, all the varieties of silk were subjected to microstructural investigation. Figure 11 depicts the X-ray diffractograms of different varieties of silk. It may be observed from the diffractograms that the mulberry varieties exhibit a broad major peak at 2θ equal to 20.5°, corresponding to (2 0 1) reflection. On the other hand, all three nonmulberry varieties show two major peaks at 2θ values of 17 and 21°, corresponding to the reflection from (0 0 2) and (2 0 1) planes. The above observations are in conformity with the results of the previous studies.[6] It is very interesting to note that although tasar, muga, and eri are genetically different, the nature of the crystals is identical, which probably depends on the ratio of alanine/glycine. The higher alanine content probably favors a distinct crystalline morphology as seen in the case of nonmulberry varieties.

To study whether there is any change in the X-ray diffraction pattern as one goes to the inner layers, WAX diffractograms were obtained for the outer, middle, and innermost layers of all the varieties (Figs. 12–16). It is quite evident from these curves that the corresponding characteristic peaks become sharper from the outer to the inner layers, indicating the development of larger crystalline regions, and also may be relatively more perfect crystals. To quantify the differences, the percentage crystallinity was calculated. Previous workers[6–8] used the formula suggested by Manjunath et al.[22] to calculate the percentage crystallinity. In the present work, an attempt was made to obtain the amorphous pattern for each variety of silk by dissolving fibers in suitable solvents and later precipitating the silk in a nonsolvent (i.e., water).

A typical diffractogram of amorphous mulberry (bivoltine) is depicted in Figure 17. Crystallinity was calculated using these curves for different silk varieties. Higher crystallinity values were observed for mulberry silks compared to those of the nonmulberry silks (Table IV). The presence of amino acids with bulky side groups in nonmulberry silks results in lower crystallinity.[1] Interestingly, all three nonmulberry silks show large crystallite size (Table V) compared to that of mulberry silks. Larger crystallites and lower crystallinity in nonmulberry varieties mean higher elongation. One may notice an increase in crystallinity and crystallite size from the outer to the innermost layers in all the varieties of silk.

It is also interesting to note the increasing trend for crystallite orientation function, from the outer to the inner layers, indicating the progressive alignment of the crystalline regions (Table VI). The increase in value is more significant in mulberry varieties than in nonmulberry silks. Both tasar and muga show similar trends. Incidentally, eri exhibits the least crystallite orientation.

TABLE XI
Correlation Coefficient *R* Value Between Initial Modulus and Microstructural Parameters

Within variety	Crystallinity (X_c)	Crystallite orientation function (f_c)	Crystallite size	Birefringence (Δ_n)	Sonic modulus (S_ε)	Dichroic ratio (D)
Mulberry (bivoltine)	0.987 (+)	0.916 (+)	0.922 (+)	0.952 (+)	0.813 (+)	0.896 (+)
Mulberry (crossbreed)	0.985 (+)	0.955 (+)	0.906 (+)	0.943 (+)	0.990 (+)	0.995 (+)
Tasar	0.978 (+)	0.975 (+)	0.964 (+)	0.982 (+)	0.875 (+)	0.951 (+)
Muga	0.885 (+)	0.926 (+)	0.937 (+)	0.933 (+)	0.955 (+)	0.937 (+)
Eri	0.885 (+)	0.957 (+)	0.987 (+)	0.825 (+)	0.937 (+)	0.893 (+)
Global	0.204 (+)	0.376 (+)	0.103 (+)	0.201 (+)	0.444 (+)	0.544 (+)

TABLE XII
Correlation Coefficient *R* Value Between Elongation and Microstructural Parameters

Within variety	Crystallinity (X_c)	Crystallite orientation function (f_c)	Crystallite size	Birefringence (Δ_n)	Sonic modulus (S_ε)	Dichroic ratio (D)
Mulberry (bivoltine)	0.981 (−)	0.949 (−)	0.950 (−)	0.936 (−)	0.802 (−)	0.930 (−)
Mulberry (crossbreed)	0.948 (−)	0.972 (−)	0.982 (−)	0.924 (−)	0.951 (−)	0.995 (+)
Tasar	0.962 (−)	0.989 (−)	0.982 (−)	0.996 (−)	0.939 (−)	0.958 (−)
Muga	0.821 (−)	0.929 (−)	0.911 (−)	0.897 (−)	0.890 (−)	0.904 (−)
Eri	0.960 (−)	0.989 (−)	0.964 (−)	0.937 (−)	0.991 (−)	0.985 (−)
Global	0.556 (−)	0.527 (−)	0.404 (−)	0.705 (−)	0.838 (−)	0.337 (−)

FTIR spectroscopy

Previous workers[7,23,24] investigated the infrared spectra of different silk fibers. The IR spectra in the range of 1400–800 cm^{-1} were found to be characteristic of individual fibroins. For mulberry silk, the bands assigned to the β-structure are 1630, 1530, 1265, and 700 cm^{-1}, corresponding to amide-I, amide-II, amide-III, and amide-V, respectively. Magoshi and Magoshi[25] reported the IR spectra of Tassah silk obtained from *Antheraea pernei* silk worm glands. The regenerated film was found to be amorphous with characteristic bands at 1660, 1550, 1310, 1270, 1107, 890, and 650 cm^{-1}. On heating, the film was converted to the β-form, showing characteristic bands at 1630, 1530, 1240, 970, and 700 cm^{-1}. The IR spectra in the case of eri and muga were found to be similar to that of tasar.

Figures 18 and 19 show the typical FTIR spectra of mulberry and eri silk fibers in the range 1400–800 cm^{-1}, as obtained in this study. In both the mulberry varieties, prominent peaks are present at 998 and 976 cm^{-1}. These bands were attributed to Gly–Aly linkages, whereas the bands at 1015 and 970 cm^{-1} were characteristic of Gly–Gly and Ala–Ala linkages.[6] Both these bands are totally absent in mulberry silks, which indicates that the formation of crystalline structure of mulberry may be more attributable to Gly–Ala linkages. However, in the case of nonmulberry silks there is a strong band at 965 cm^{-1}, characteristic of Ala–Ala linkage, suggesting the formation of crystalline structure based on Ala–Ala linkage in these fibers.

Dichroic ratio

A glance at the typical spectra of mulberry and eri shows very significant differences in bands at 998 and 976 cm^{-1} for mulberry (bivoltine) and at 965 cm^{-1} for eri, when the polarizer angle was changed from 0 to 90°. The absorbance ratios at these peaks can provide a fairly good idea of molecular orientation in these fibers. The spectrum of mulberry (crossbreed) was similar to that of mulberry (bivoltine), whereas those of tasar and muga were similar to that of eri. To obtain a quantitative idea of molecular orientation, the dichroic ratios ($A_\parallel/A_\perp$) were calculated at 998 and 976 cm^{-1} for the mulberry varieties and at 965 cm^{-1} for the nonmulberry varieties.

Dichroic ratio values, reported in Table VII, indicate an increasing trend from the outer layer to the innermost layers within a cocoon for both mulberry and nonmulberry silks. Among the five varieties, mulberry (bivoltine) shows the highest value and eri the least. These results support our earlier observations on crystallite orientation, suggesting a possible improvement in the molecular chain orientation as one approach from the outer to the innermost layers. For instance, in the mulberry (bivoltine) variety a good positive correlation was observed between the dichroic ratio and the physical properties, such as tenacity ($r = 0.980$) and initial modulus ($r = 0.896$). On the other hand, elongation shows a good negative correlation ($r = 0.930$). Similar results were also obtained in other varieties (Table VIII).

Birefringence and sonic modulus

The birefringence (Δ_n) value gives an idea about the overall molecular orientation, whereas the sonic modulus ($S_\in$) gives a combined effect of order and orientation. The values of Δ_n and $S_\in$ are listed in Tables VIII and IX, respectively. As was observed with f_c and D values, the birefringence and sonic modulus increase from the outer to the inner layers within the same variety. This trend was observed in all varieties. For

TABLE XIII
Rate of Change of Load at 85% of Maximum Attainable Stress Change (R_{85})

	0% Retraction		80% Retraction	
Variety	Outer layer	Inner layer	Outer layer	Inner layer
Mulberry (bivoltine)	−0.67	−0.17	0.78	0.28
Mulberry (crossbreed)	−0.88	−0.26	0.61	0.34
Tasar	−2.76	−1.57	1.12	0.57
Muga	−1.16	−0.64	1.02	0.47
Eri	0.99	−0.49	1.06	0.33

TABLE XIV
Correlation Coefficient (*r*) Between Physical Structural Parameters and the Rate of Change of Tension $|R_{85}|$

Global	Crystallinity	Crystallite orientation	Birefringence	Sonic modulus	Dichroic ratio
0% retraction	0.912 (−)	0.875 (−)	0.713 (−)	0.698 (−)	0.853 (−)
80% retraction	0.936 (−)	0.847 (−)	0.729 (−)	0.787 (−)	0.836 (−)

instance, for the mulberry (bivoltine) variety, a good positive correlation was observed between tenacity and birefringence ($r = 0.869$) and initial modulus and birefringence ($r = 0.952$), and a negative correlation between elongation and birefringence ($r = 0.936$) and the sonic modulus ($r = 0.802$). Similarly, for the same variety a moderate-to-good positive correlation was found between tenacity and sonic modulus ($r = 0.690$) and between initial modulus and sonic modulus ($r = 0.813$). With elongation, however, a negative correlation was observed with sonic modulus ($r = 0.802$). Similar values were observed with other varieties with respect to the change within the same variety (Table X). This clearly established that the morphological structure plays a predominant role in determining the mechanical properties of silk fibroin, irrespective of variety.

To understand the effect of these parameters on mechanical properties, correlations between tenacity, elongation, and initial modulus values and various microstructural parameters within a variety were determined. A good positive correlation was observed between tenacity, initial modulus, and crystallinity, crystallite orientation function, and crystallite size. For instance, for the mulberry (bivoltine) variety, high positive correlations were found between tenacity and crystallite orientation function ($r = 0.913$), tenacity and crystallinity ($r = 0.92$), and tenacity and crystallite size ($r = 0.961$) (Table X). Similarly, the correlations were positive for initial modulus with crystallinity ($r = 0.987$) and initial modulus with crystallite orientation function ($r = 0.916$) (Table XI). On the other hand, negative correlations were observed between elongation and crystallinity ($r = 0.981$) and elongation and crystallite orientation function ($r = 0.949$). A similar trend was observed for nonmulberry varieties of silk (Table XII), suggesting that an increase in the abovementioned structural parameters promotes an increase in the tenacity and initial modulus and a decrease in elongation values from the outer to the inner layers. Silk filament is spun by joint forces of drawing (from outside) and ejection (from inside), which are accompanied by shearing stresses acting on aqueous silk. It crystallizes to form fibers more easily in less-concentrated solutions.[4] This strongly suggests that the silk filaments become more ordered and more crystalline as they become thinner.

With respect to stress relaxation, it is clear that morphology of the fiber does play a very significant role in governing the relaxation behavior. The inner layers behave differently than the outer layers, also with respect to different varieties. It was considered of considerable interest if one could establish a correlation between the relaxation parameter Ri and the various morphological characteristics of the silk fibers, irrespective of the nature of fiber. Surprisingly, the global correlation—taking all the samples together—did not provide any significant and meaningful correlation with various microstructural parameters such as crystallinity, orientation, birefringence, and so forth. Therefore, it was decided to compare the rate of change of tension. Two such parameters were determined:

1. R_{85}, defined as the ratio of 85% tension relaxed and built up to the time (in s) taken to achieve this value of stress (i.e., $\Delta T_{85}/\Delta t_{85}$). The values are given in Table XIII.
2. Rt_2, defined as the slope of the curve at t_2 (i.e., $\delta T/\delta t$, where T and t are negligible).

It is evident from Table XIII that the rate R_{85} for the relaxation phenomenon (i.e., at 0% retraction) is negative, whereas that for inverse stress relaxation (i.e., at 80% retraction) is positive. The rate (R_{85}) for inner layers has a lower magnitude, and the rate (R_{85}) for the nonmulberry variety is higher than that for mulberry.

It is very interesting to find regarding the global correlation coefficient (R) between R_{85} and various morphological parameters that, irrespective of the nature of silk, the correlations are very high and give

TABLE XV
Rate of Change of Load at t_2 (Rt_2)

	0% Retraction		80% Retraction	
Variety	Outer layer	Inner layer	Outer layer	Inner layer
Mulberry (bivoltine)	−3.75	−2.54	2.64	1.85
Mulberry (crossbreed)	−3.95	−2.96	2.74	1.93
Tasar	−6.17	−5.28	3.77	3.17
Muga	−3.89	−3.58	3.45	2.37
Eri	−4.45	−3.86	2.37	1.85

TABLE XVI
Correlation Coefficient (*R*) Between Physical Structural Parameters and the Rate of Change of Tension at t_2 $|Rt_2|$

Global	Crystallinity	Crystallite orientation	Birefringence	Sonic modulus	Dichroic ratio
0% retraction	0.946 (−)	0.913 (−)	0.879 (−)	0.885 (−)	0.894 (−)
80% retraction	0.957 (−)	0.935 (−)	0.923 (−)	0.876 (−)	0.898 (−)

negative value, signifying that the higher the value, the lower the $|R_{85}|$. This is true at both 0% retraction (classical stress relaxation experiment) and at 80% (inverse stress relaxation experiment) (Table XIV).

Similarly, Rt_2 values were calculated and are tabulated in Table XV, where it may be seen that the trends are similar. Correlation coefficients obtained with $|Rt_2|$ and morphological parameters at 0 and 80% retraction levels are given in Table XVI. One may note that these values are higher compared to those obtained with $|R_{85}|$. This rate is thus a more sensitive parameter. The above discussion strongly suggests that the stress relaxation and inverse stress relaxation phenomena are truly dependent on structure. In addition, because the molecular relaxation is a time-dependent process, the rate parameters $|R_{85}|$ and $|Rt_2|$ thus show excellent correlation.

General correlations

The above discussion has clearly demonstrated the importance of structure in determination of tensile properties of silk fibers. Within the same variety, the various microstructural parameters have shown very good correlation. It was considered of interest, however, to find whether a generalized global correlation between the properties and the structural parameters exists, irrespective of the nature, type, and position of the filament. It was surprising to note that a generalized overall correlation between mechanical properties and various microstructural parameters, although suggesting correct trends, was not good—except in some cases that obviously prove the rule that such trends may not go beyond a point. What this means is that between the different varieties such correlations are difficult to establish because the chemical architecture changes significantly; for example, ratios of amino acids with bulky side groups/nonbulky side groups are quite different in mulberry and nonmulberry varieties. Ratios are higher for nonmulberry (0.24–0.30) than for mulberry varieties (0.17–0.18). Bulkier groups obviously hamper development of good morphology and this change may not follow the changes in microstructure. Similarly, a higher alanine content led to a different crystalline structure.

It was pointed out earlier in this study that the X-ray diffraction pattern and the IR spectra of both mulberry varieties are similar to each other and those of the nonmulberry varieties are similar to each other. The chemical architecture also more or less points toward these similarities.

Keeping this in view, global correlations for mulberry and nonmulberry varieties were compared separately. It was interesting to note that the correlations between mechanical properties and microstructure are very high within these groups, except in some cases, which proves the rule (Table XVII).

In this respect, mulberry and nonmulberry seem to represent different classes. In addition, despite genetically different profiles, the tasar, muga, and eri behave quite similarly to each other, with chemical architectures showing very good similarities.

CONCLUSIONS

Irrespective of the variety, the mechanical properties significantly changed from the outer to the inner layers within a variety, for instance, tenacity and modulus increased while elongation decreased. The two phenomena, the stress relaxation and the inverse stress relaxation, simultaneously represent the molecular relaxation in the retracted fiber. At low retraction

TABLE XVII
Correlation Coefficient *R* Value Between Properties and Microstructural Parameters (Global)

	Tenacity			Initial modulus		
Variety	Crystallinity	Crystallite size	Crystallite orientation function	Crystallinity	Crystallite size	Crystallite orientation function
Mulberry	0.987 (+)	0.964 (+)	0.962 (+)	0.975 (+)	0.941 (+)	0.933 (+)
Nonmulberry	0.988 (+)	0.918 (+)	0.974 (+)	0.337 (+)	0.968 (+)	0.942 (+)

levels, the former predominated, giving negative values of the Ri, and at higher levels the inverse stress relaxation predominated, leading to positive values of the Ri. Similarly, all the microstructural parameters showed significant increases from the outer to the inner layers. These changes correlated very well with properties within a variety. However, a global correlation taking all the varieties did not give good correlation values because of the substantial differences in chemical architecture in the mulberry and nonmulberry varieties. However, when parameter correlations for these two groups were computed separately, very good correlations were observed between structure and properties. In this respect, the nonmulberry varieties behaved in a similar manner, despite different genetic profiles.

References

1. Sen, K.; Babu K, M. J Appl Polym Sci, to appear.
2. Iizuka, E.; Kawano, R.; Kitani, Y.; Okachi, Y.; Shimizu, M.; Fukuda, A. Indian J Seric 1993, 32, 27.
3. Iizuka, E.; Okachi, Y.; Shimizer, M.; Fukuda, A.; Hashizume, M. J Seric 1993, 1, 1.
4. Iizuka, E.; Okachi, Y.; Shimizer, M.; Fukuda, A.; Hashizume, M. Indian J Seric 1993, 32, 175.
5. Iizuka, E.; Teramoto, A.; Lu, Q.; Miu, S.-S.; Shimizu, O. J Seric Sci Jpn 1996, 65, 134.
6. Bhat, N. V.; Nadiger, G. S. J Appl Polym Sci 1980, 25, 921.
7. Bhat, N. V.; Ahirrao, S. M. J Polym Sci 1983, 21, 1273.
8. Bhat, N. V.; Ahirrao, S. M. Text Res J 1985, 55, 65.
9. Nachane, R. P.; Hussain, G. F. S.; Krishna Iyer, K. R. Text Res J 1982, 52, 483.
10. Nachane, R. P.; Hussain, G. F. S.; Patel, G. S.; Krishna Iyer, K. R. J Appl Polym Sci 1989, 38, 21.
11. Nachane, R. P.; Hussain, G. F. S.; Patel, G. S.; Krishna Iyer, K. R. J Appl Polym Sci 1986, 31, 1101.
12. Manich, A. M.; De Castellar, M. D. Text Res J 1992, 62, 196.
13. Vangheluwe, L. Text Res J 1993, 63, 552.
14. Peters, L.; Woods, H. J. In: Mechanical Properties of Textile Fibres; Meredith, R., Ed.; North-Holland: Amsterdam, 1956.
15. Bhuvanesh, Y. C.; Gupta, V. B. Polymer 1995, 36, 3669.
16. Das, S. Ph.D. Thesis, Indian Institute of Technology, Delhi, 1996.
17. Alexander, L. E. X-ray Diffraction Methods in Polymer Science; Wiley–Interscience: New York, 1969.
18. Iizuka, E. J Appl Polym Sci Appl Polym Symp 1985, 41, 173.
19. Iijuka, E.; Itoh, H. Int J Wild Silkmoth Silk 1997, 3, 37.
20. Freddi, G.; Gotoh, Y.; Mori, T.; Tsutsui, I.; Tsukada, M. J Appl Polym Sci 1994, 52, 775.
21. Iizuka, E.; Vegaki, K.; Takamatsu, H.; Okachi, Y.; Kawai, E. J Seric Sci Jpn 1994, 63, 64.
22. Manjunath, B. R.; Venkataraman, A.; Stephen, T. J Appl Polym Sci 1973, 17, 1091.
23. Baruah, G. C.; Talukdar, C.; Bora, M. N. Indian J Phys 1991, 65B, 651.
24. Magoshi, J.; Magoshi, Y. J Polym Sci 1977, 15, 1675.
25. Magoshi, J.; Magoshi, Y. J Polym Sci 1975, 13, 1347.